Analysis of radiatively stable entanglement in a system of two dipole-interacting three-level atoms

I. V. Bargatin, B. A. Grishanin, and V. N. Zadkov
International Laser Center and Department of Physics, M. V. Lomonosov Moscow State University, Moscow 119899, Russia
(Received 29 November 1999; published 7 April 2000)

We explore the possibilities of creating radiatively stable entangled states of two three-level dipole-interacting atoms in a Λ configuration by means of laser biharmonic continuous driving or pulses. We propose three schemes for generation of entangled states which involve only the lower states of the Λ system, not vulnerable to radiative decay. Two of them employ coherent dynamics to achieve entanglement in the system, whereas the third one uses optical pumping, i.e., an essentially incoherent process.

PACS number(s): 03.67.−a, 32.80.Qk, 03.65.Bz

I. INTRODUCTION

The concept of quantum entanglement, one of the most intriguing properties of multipartite quantum systems [1], has been intensively exploited over the last decade in connection with quantum information processing. It has been shown that the use of entangled states opens new horizons in such practical fields as cryptography [2], computing [3], information transmission [4], and precision measurement [5]. However, all of these applications become possible only with a reliable source of entanglement. Traditionally, entangled particles have been generated in the down-conversion nonlinear process [6,7], but this method is in some cases disadvantageous due to the speedy nature of the produced particles (photons) and the intrinsic randomness of their appearance times. That is why efforts are now being made to find ways for controlled production of entangled states of less volatile massive particles [8]. During the last few years, various methods for creation of entangled states of atoms, ranging from continuous observation of radiative decay [9,10] to controlled cold collisions [11], have been proposed and some of them experimentally demonstrated [12,13].

Though the resonant dipole-dipole interaction (RDDI) was suggested for realization of entangling dynamics as early as 1995 [14], it was only recently that several authors [15–17] investigated this interaction in more detail as a method for entangling neutral atoms in optical traps (neutral atom realizations benefit from the fact that neutral atoms are less sensitive to stray EM fields—a major source of decoherence in ions [18]). While the authors of Ref. [15] offered qualitative arguments for realization of this idea in dipole traps [19], Refs. [16], [17] considered quantitative models of creation of maximally entangled states of two-level atoms. Unfortunately, such entangled states of two-level atoms have short lifetimes due to radiative decay. Obviously, since radiative decay and the RDDI have the same physical nature, we cannot avoid the former while making use of the latter. In this paper we solve this conceptual problem by presenting methods for creation of radiatively stable entanglement in a system of dipole-interacting three-level atoms. Though the model considered here is still far from representing the real situations (see [20] for details of a possible experimental realization), it offers insights into how the RDDI can be used to entangle real, multilevel atoms.

II. THE MODEL

Extending the model described in [16], we consider here two identical three-level atoms in a Λ configuration (Fig. 1) fixed at a distance R. The dipole transitions $|1\rangle\leftrightarrow|3\rangle$ and $|2\rangle\leftrightarrow|3\rangle$ of both atoms are driven by two near-resonant laser fields. Taking the two limiting cases, we consider only two types of geometry: when the laser fields are either perpendicular or parallel to the radius vector $\vec{R}$ connecting the atoms (these geometries are shown in Fig. 2 and identified as symmetric and antisymmetric, respectively). Within the interaction picture and rotating wave approximation, the evolution of the system interacting with the laser fields is governed by the following master equation [21]:

$$\frac{\partial\hat{\rho}}{\partial t}=-\frac{i}{\hbar}[\hat{\mathcal{H}}_{\mathrm{eff}},\hat{\rho}]+\sum_{i,j,k=1,2}\frac{\gamma_{k3}^{(ij)}}{2}(2\hat{\sigma}_{3k}^{(i)}\hat{\rho}\hat{\sigma}_{k3}^{(j)}-\hat{\rho}\hat{\sigma}_{3k}^{(i)}\hat{\sigma}_{k3}^{(j)}-\hat{\sigma}_{3k}^{(i)}\hat{\sigma}_{k3}^{(j)}\hat{\rho}), \tag{1}$$

where the upper indices i and j number the atoms, the lower ones $k3$ and $3k$ $(k=1,2)$ refer to dipole transitions of the atoms, and $\sigma_{kl}^{(i)}$ denotes the Heisenberg transition operators from level $|k\rangle$ to level $|l\rangle$ within the ith atom. Relaxation effects in the system are characterized by the single-atom decay rates, $\gamma_{k3}=\gamma_{k3}^{(11)}=\gamma_{k3}^{(22)}$, which correspond to the conventional radiative decay into free space, and the photon ex-

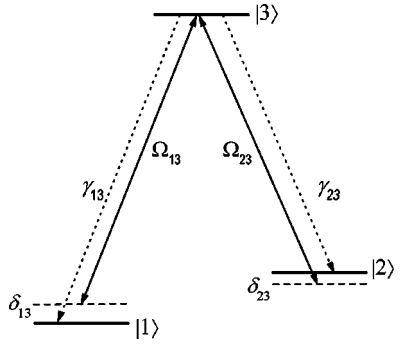

FIG. 1. The level structure of an isolated three-level atom in a Λ configuration. The dipole transitions $|1\rangle\leftrightarrow|2\rangle$ and $|2\rangle\leftrightarrow|3\rangle$ are driven by two laser fields, which are detuned by δ_{13} and δ_{23}, respectively. Dotted lines show radiative decay channels and their corresponding rates.

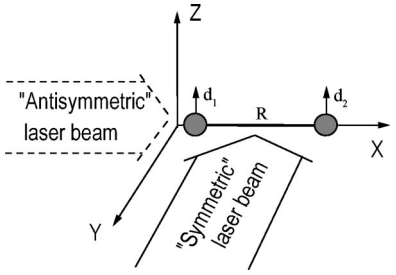

FIG. 2. Geometry of the model with directions of laser beams for the ''symmetric'' and ''antisymmetric'' laser beams.

change rates, $\gamma_{k3}^{(12)}=\gamma_{k3}^{(21)}$, which describe collective relaxation, a well-known companion of the RDDI. The effective Hamiltonian $\hat{\mathcal{H}}_{\text{eff}}$ includes interaction with the laser field and the RDDI coupling on both transitions:

$$\hat{\mathcal{H}}_{\text{eff}}=\hbar\sum_{i,k=1,2}\left(\delta_{k3}\hat{n}_k^{(i)}+\frac{\Omega_{k3}^{(i)}}{2}\hat{\sigma}_{k3}^{(i)}+\chi_{k3}\hat{\sigma}_{k3}^{(1)}\hat{\sigma}_{3k}^{(2)}+\text{H.c.}\right), \tag{2}$$

where $\hat{n}_k^{(i)}$ stands for the population operator of the level $|k\rangle$ in the ith atom, δ_{k3} are the detunings of the laser field frequencies from the corresponding transitions $|k\rangle\leftrightarrow|3\rangle$ of an isolated atom, $\Omega_{k3}^{(i)}$ is the Rabi frequency of the laser field acting on the $|k\rangle\leftrightarrow|3\rangle$ transition of the ith atom, and χ_{k3} is the RDDI coupling strength on the $|k\rangle\leftrightarrow|3\rangle$ transition. Throughout the rest of this paper we will consider the case of wide homogeneous laser beams, so that the Rabi frequencies acting on the two atoms may differ in phase but not in magnitude, $|\Omega_{k3}^{(1)}|=|\Omega_{k3}^{(2)}|$.

Normalizing the RDDI parameters χ_{k3}, $\gamma_{k3}^{(12)}$, and $\gamma_{k3}^{(21)}$ by the decay rate of an isolated atom, γ_{k3}, we introduce the dimensionless parameters

$$g_{k3}=\gamma_{k3}^{(12)}/\gamma_{k3}=\gamma_{k3}^{(21)}/\gamma_{k3},\quad f_{k3}=\chi_{k3}/\gamma_{k3}, \tag{3}$$

which are given by the following expressions [21]:

$$\begin{aligned}f_{k3}=F(\varphi_{k3})=&\frac{3}{2}\left(\frac{\cos\varphi_{k3}}{\varphi_{k3}^3}+\frac{\sin\varphi_{k3}}{\varphi_{k3}^2}-\frac{\cos\varphi_{k3}}{\varphi_{k3}}\right)\\&\times[\vec{e}_1\cdot\vec{e}_2-(\vec{e}_1\cdot\vec{e}_R)(\vec{e}_2\cdot\vec{e}_R)]-3\left(\frac{\cos\varphi_{k3}}{\varphi_{k3}^3}+\frac{\sin\varphi_{k3}}{\varphi_{k3}^2}\right)\\&\times[(\vec{e}_1\cdot\vec{e}_R)(\vec{e}_2\cdot\vec{e}_R)],\\g_{k3}=G(\varphi_{k3})=&\frac{3}{2}\left(\frac{\sin\varphi_{k3}}{\varphi_{k3}}+\frac{\cos\varphi_{k3}}{\varphi_{k3}^2}-\frac{\sin\varphi_{k3}}{\varphi_{k3}^3}\right)\\&\times[\vec{e}_1\cdot\vec{e}_2-(\vec{e}_1\cdot\vec{e}_R)(\vec{e}_2\cdot\vec{e}_R)]+3\left(\frac{\sin\varphi_{k3}}{\varphi_{k3}^3}-\frac{\cos\varphi_{k3}}{\varphi_{k3}^2}\right)\\&\times[(\vec{e}_1\cdot\vec{e}_R)(\vec{e}_2\cdot\vec{e}_R)],\end{aligned} \tag{4}$$

where $\vec{e}_i$ $(i=1,2)$ is the unit vector in the direction of the dipole moment matrix element of the corresponding transition $|k\rangle\leftrightarrow|3\rangle$ of the ith atom, $\vec{e}_R$ is the unit vector in the direction of $\vec{R}$, and $\varphi_{k3}=k_{k3}R$ is the dimensionless distance between the atoms ($k_{k3}=\omega_{k3}/c$ is the wave number associated with the transition $|k\rangle\leftrightarrow|3\rangle$ of an isolated atom). Throughout the following discussion we will assume, for the sake of simplicity, that the dipole moments are real, collinear with each other, and perpendicular to the radius vector $\vec{R}$ (other dipole moment orientations lead to qualitatively the same results).

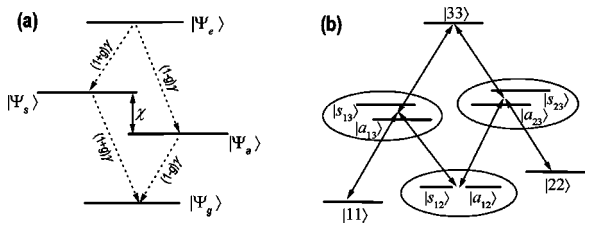

FIG. 3. (a) Energy levels of two dipole-interacting two-level atoms (Dicke states). The two maximally entangled Dicke states $|\Psi_a\rangle$ and $|\Psi_s\rangle$ are split by the RDDI coupling strength χ. Also shown in the figure are the radiative decay channels with the corresponding decay rates. (b) The same for two dipole-interacting Λ systems. Shown are the doublets, formed by symmetric and antisymmetric Dicke-like states, and the laser-induced transitions induced by the two components of the biharmonic driving.

In the case of two-level atoms, the simplest description of the system dynamics is offered by the basis of the Dicke states, which is formed by the doubly excited state $|\Psi_e\rangle=|e\rangle_1|e\rangle_2$, the ground state $|\Psi_g\rangle=|g\rangle_1|g\rangle_2$, and the two singly excited maximally entangled states—the symmetric $|\Psi_s\rangle=(1/\sqrt{2})(|g\rangle_1|e\rangle_2+|e\rangle_1|g\rangle_2)$ and the antisymmetric one $|\Psi_a\rangle=(1/\sqrt{2})(|g\rangle_1|e\rangle_2-|e\rangle_1|g\rangle_2)$ [the corresponding energy diagram is shown in Fig. 3(a)]. For the case of three-level atoms considered here it is useful to introduce simple generalizations of the Dicke states. The role of the ground and doubly excited Dicke states is then played by the three tensor product states $|kk\rangle=|k\rangle_1|k\rangle_2, k=1,2,3$, while the symmetric and antisymmetric Dicke states now are represented by the three symmetric and three antisymmetric maximally entangled states $|s_{kl}\rangle=(1/\sqrt{2})(|k\rangle_1|l\rangle_2+|k\rangle_1|l\rangle_2)$ and $|a_{kl}\rangle=(1/\sqrt{2})(|k\rangle_1|l\rangle_2-|k\rangle_1|l\rangle_2)$, $k,l=1,2,3, k<l$. The corresponding energy diagram is shown in Fig. 3(b). Note that in both two- and three-level models the energy levels can be grouped according to their type of symmetry: the unentangled states $|kk\rangle=|k\rangle_1|k\rangle_2$, as well as the states $|s_{kl}\rangle=(1/\sqrt{2})(|k\rangle_1|l\rangle_2+|k\rangle_1|l\rangle_2)$, can be said to belong to one type of symmetry (symmetric with respect to the atom interchange), and the states $|a_{kl}=(1/\sqrt{2})(|k\rangle_1|l\rangle_2+|k\rangle_1|l\rangle_2)$ to another (antisymmetric with respect to the atom interchange). The transitions between these levels can then be classified as symmetry preserving and symmetry breaking, respectively. It is easy to show that, due to the form of the transition matrix elements, the symmetry-preserving transitions are sensitive only to the sum of the Rabi frequencies, $\Omega_{k3}^{(1)}+\Omega_{k3}^{(2)}$, acting on the atoms, and the symmetry-breaking transitions only to their difference, $\Omega_{k3}^{(1)}-\Omega_{k3}^{(2)}$.

In the following, we also assume that the system is initially stored in the $|11\rangle$ state, which can easily be achieved by conventional optical pumping methods [22].

III. COHERENT ENTANGLING PROCESSES

A. Resonant Raman pulses

In our previous paper [16] we have shown that the maximally entangled Dicke states $|\Psi_s|$ or $|\Psi_a\rangle$ of two two-level atoms can be efficiently populated at small interatomic distances simply by applying an appropriately tailored laser pulse. Assuming that initially the entire population of the system is concentrated in the ground state $|\Psi_g\rangle$, this pulse should be tuned into resonance with a transition to only one of these maximally entangled states. Then, by applying a π-pulse analog, a significant part of the population of the system can be transferred to one of these states, thereby creating entanglement in the system. We have also shown that the entanglement fidelity, defined as the population of the corresponding maximally entangled state, can be made arbitrarily close to unity as the interatomic distance R goes to zero.

In this paper we propose ways to create stable entanglement in a system of two three-level atoms. To be radiatively stable, the created entangled states should involve only the lower levels $|1\rangle$ and $|2\rangle$ of the original Λ system of each atom, as only these states are not vulnerable to radiative decay. Therefore, our goal here will be to achieve the maximum possible population of one of the maximally entangled states $|a_{12}\rangle$ or $|s_{12}\rangle$ [see Fig. 3(b)]. The most straightforward way to do this is to extend the results of the two-level model to the three-level one, considered here, by using resonant Raman pulses. By the latter we mean a sequence of two coherent π pulses, the first of which transfers the population to one of the maximally entangled states involving the initial lower level of the Λ system and some quickly decaying upper lying ''transit'' level, while the second one transfers the entire population of the ''transit'' level to another radiatively stable lower level of the Λ system, thus removing the radiative instability of the entanglement.

In the considered system of two dipole-interacting three-level atoms, the role of the intermediate ''transit'' state can be played by the above-mentioned levels $|a_{13}\rangle$ or $|s_{13}\rangle$ (one should not forget that the system is initially in the state $|11\rangle$). During the first step, the pulse resonant, for example, with the $|11\rangle \leftrightarrow |s_{13}\rangle$ transition transfers the population to the maximally entangled state $|s_{13}\rangle$; the second step creates the radiatively stable maximally entangled state $|s_{12}\rangle$ by application of the symmetry-preserving π pulse resonant with the $|s_{13}\rangle \leftrightarrow |s_{12}\rangle$ transition. In fact, it is the symmetry preservation rules that prevent population from going into the $|a_{13}\rangle$ state in a transition that is also resonant with the second pulse.

For both pulses to be resonant, the parameters of the laser field should be chosen in the following way:

$$\alpha_{k3}=0, \quad \delta_{k3}=\chi_{13}/2, \quad |\Omega_{k3}^{(i)}| \ll |\chi_{13}|, \tag{5}$$

where α_{k3} is the phase difference between the Rabi frequencies acting on the two atoms, $\Omega_{k3}^{(1)}=\Omega_{k3}^{(2)}\exp(i\alpha_{k3})$ (considering laser beams formed by traveling waves, α_{k3} varies from zero for the symmetric geometry to φ_{k3} for the antisymmetric one, and takes all the intermediate values for other types of laser field geometry). The parameters given by Eq. (5) correspond therefore to the case when both lasers are used in the symmetric geometry, the ''transit'' state is $|s_{13}\rangle$, and the final radiatively stable maximally entangled state is $|s_{12}\rangle$. Other types of geometries and laser parameter sets can obviously be chosen when using the other intermediate state $|a_{13}\rangle$ and/or creating the other radiatively stable maximally entangled state $|a_{12}\rangle$. For example, to create the $|a_{12}\rangle$ state, one can use the following set of parameters:

$$\alpha_{13}=\varphi_{13}, \quad \alpha_{23}=0, \quad \delta_{k3}=-\chi_{13}/2, \quad |\Omega_{k3}^{(i)}| \ll |\chi_{13}|. \tag{6}$$

The phase differences α_{k3} in this case correspond to one of the laser beams being used in the antisymmetric geometry, and the other in the symmetric one. Note that, when using antisymmetric geometry at small interatomic distances ($\varphi_{k3} \ll 1$), most of the laser power is ''wasted'' since only a fraction of it contributes to the corresponding transition matrix element $|\langle 11|\hat{\mathcal{H}}_{\rm eff}/\hbar|a_{13}\rangle| = |\Omega_{13}^{(1)}-\Omega_{13}^{(2)}|/2 = |\Omega_{13}^{(i)}|\sin(\varphi_{13}/2) \ll |\Omega_{13}^{(i)}|$, and actually induces transitions $|11\rangle \leftrightarrow |a_{13}\rangle$.

While a simple estimate of the resulting fidelity of creation of the maximally entangled state is offered by a product of the fidelities of each step of the resonant Raman process (which were calculated in [16] within the two-level atom model), rigorous results can be obtained only by explicit solution of the corresponding master equation. Due to the high dimensionality of the master equation (1), this calculation is rather demanding computationally, and was not included in the present treatment.

B. Stimulated Raman adiabatic passage

Another coherent method for creation of maximally entangled states is based on the stimulated Raman adiabatic passage (STIRAP) technique [23], a well-known alternative to Raman pulses. The STIRAP method uses adiabatic following of the system state after the slowly changing parameters of the laser field, which are chosen to form a so-called counterintuitive pulse sequence. The STIRAP technique benefits from extremely low probabilities of losing coherence due to radiative decay of the intermediate states, and has already been proposed for use in entanglement-related problems [24]. In our case, efficient transfer of the population from the state $|11\rangle$ to the state $|a_{12}\rangle$ or $|s_{12}\rangle$ may be deterred by existence of several intermediate states [25]. However, as we show below, efficient transfer is still possible for appropriately chosen laser pulse parameters.

To realize STIRAP in our system we need to choose the frequencies and geometries of the two constituent laser pulses in a way that would leave active (i.e., resonant and having strong transition amplitudes due to the use of the corresponding geometries; see Sec. II) only two transitions in the whole system. An appropriate choice is given by

$$\alpha_{13}=0, \quad \alpha_{23}=\pi, \quad \delta_{k3}=\chi_{13}/2, \quad \max_t |\Omega_{k3}^{(i)}| = \Omega_0 \ll |\chi_{13}|, \tag{7}$$

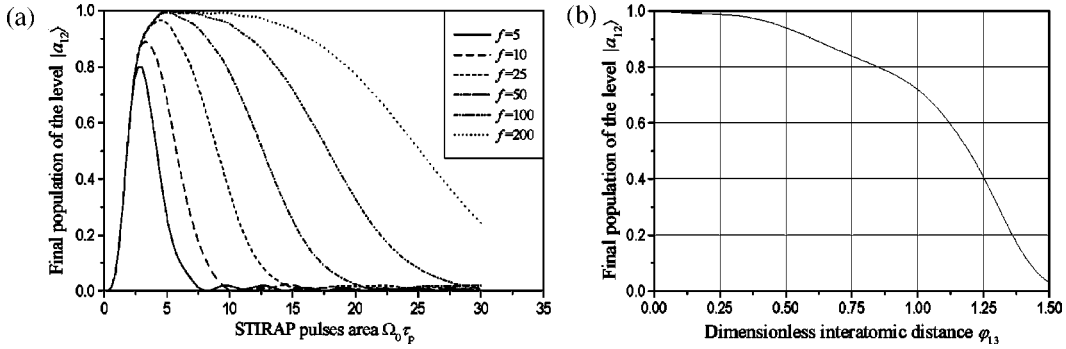

FIG. 4. (a) Population of the maximally entangled state $|a_{12}\rangle$ after adiabatic passage versus the pulse area for different values of the RDDI parameter $f=f_{13}=\chi_{13}/\gamma_{13}$. (b) The same for the optimal value of the laser pulses area, $\Omega_0\tau_p$, versus the interatomic distance φ_{13}. In both graphs we assume equal decay rates of the two channels of the original Λ system, $\gamma_{13}=\gamma_{23}$.

where Ω_0 stands for the amplitude of the corresponding constituents of the counterintuitive laser pulse sequence. The condition $\alpha_{23}=\pi$, which is very important as it prevents leakage of population into other levels, can easily be realized by using two laser beams in antisymmetric geometry, which form a standing wave with one of the nodes situated exactly in the middle of the vector $\vec{R}$ connecting the two atoms [17]. In this case only two transitions, $|11\rangle\leftrightarrow|s_{13}\rangle$ and $|s_{13}\rangle\leftrightarrow|a_{13}\rangle$, are active, and the adiabatic passage results in transfer of the total population to the radiatively stable state $|a_{13}\rangle$.

We have numerically calculated the final population (fidelity) of the state $|a_{12}\rangle$ after the STIRAP procedure by explicit solution of the corresponding Schrödinger equation with the Hamiltonian given by Eq. (2). The two laser field pulses had the same Gaussian form and were delayed with respect to each other by their length [23], and the rest of the parameters were given by Eq. (7). For determinacy, the length of the pulses was chosen to be equal to one-tenth of the lifetime of the excited level $|3\rangle$ of the original Λ system, $\tau_p=0.1/(\gamma_{13}+\gamma_{23})$. The final population of the level $|a_{12}\rangle$ is shown in Fig. 4(a) as a function of the pulse Rabi frequency amplitude Ω_0 for different values of the RDDI splitting parameter f_{13}. As one can see from the figure, for sufficiently high RDDI splittings (i.e., for sufficiently small atomic separations) the fidelity first grows with increasing Ω_0, reaching saturation at $\Omega_0\tau_p\approx 5$, which corresponds to the adiabaticity condition on the pulse area [23]. Then, after some point, the final inequality in Eq. (7) is no longer fulfilled and the efficiency of the process degrades due to nonresonant excitation of other levels caused by power broadening. For the same reasons, the fidelity does not reach unity at any values of Ω_0 for low RDDI splittings (large interatomic separations). In Fig. 4(b) we show the overall fidelity of the STIRAP method for optimized values of the Rabi frequency amplitude as a function of the interatomic distance φ_{13}.

As we ignore relaxation processes in this model (a common practice for STIRAP simulations), one should beware of relaxation-induced errors. However, these errors assume significant values only for the case of long pulses, $\tau_p\geqslant 1/(\gamma_{13}+\gamma_{23})$, and low overall STIRAP process fidelity, i.e., situations that are not of great concern to us here.

IV. AN INCOHERENT ENTANGLING PROCESS: OPTICAL PUMPING

An interesting alternative to the coherent methods can be offered by optical pumping schemes where the stationary state of the system corresponds to one of the maximally entangled states. In this situation, the population of the system is pumped into the entangled state after asymptotically large time periods.

Consider the following choice of the laser field parameters:

$$\alpha_{k3}=0, \quad \delta_{k3}=\chi_{13}/2, \quad |\Omega_{k3}|\ll|\chi_{k3}|. \tag{8}$$

Neglecting nonresonant excitation at small interatomic distances, only a few transitions remain resonant and have the corresponding geometry. These active transitions are shown in Fig. 5(a) (the upper state $|33\rangle$ is omitted in the figure, as it

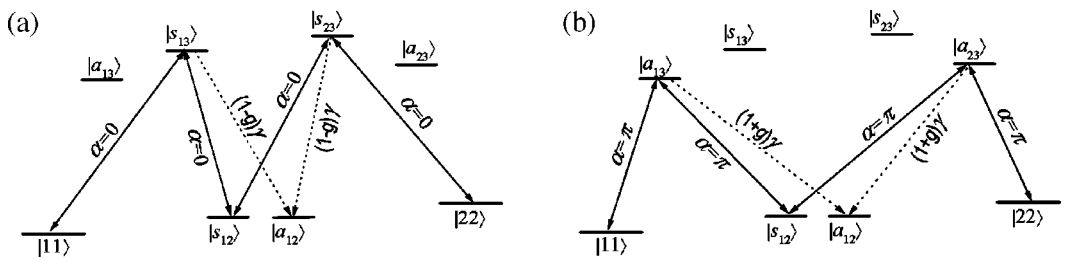

FIG. 5. Energy-level diagram and transitions for two variants, symmetric (a) and antisymmetric (b), of the optical pumping scheme. Solid lines indicate laser-induced transitions with the corresponding phase differences α between two atoms. Dotted lines show the significant decay channels with the corresponding decay rates. The negligibly populated upper state $|33\rangle$ is omitted in both figures.

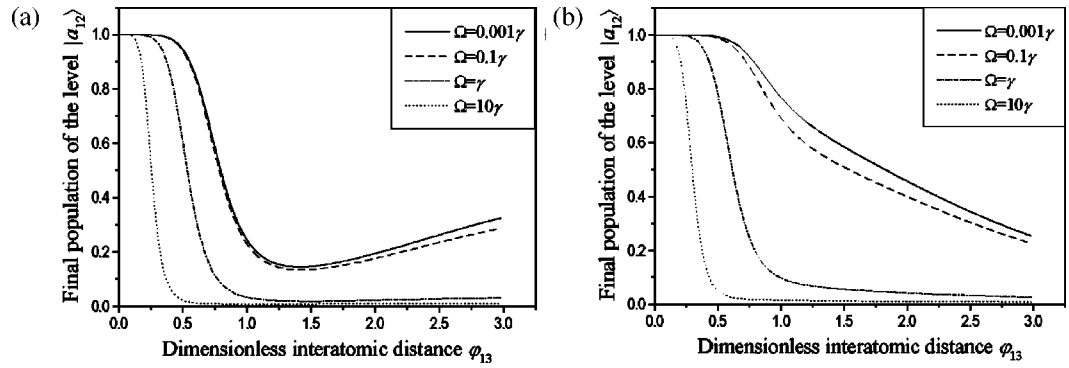

FIG. 6. Population of the maximally entangled state $|a_{12}\rangle$ in the stationary solution of the master equation as a function of the interatomic distance φ_{13}, for different values of the Rabi frequencies $|\Omega_{k3}^{(i)}|=\Omega$, i, $k=1$, 2 and the two discussed geometries, symmetric (a) and antisymmetric (b).

is only negligibly excited at small interatomic distances [16]). As seen from the figure, the maximally entangled state $|a_{12}\rangle$ is not included in the chain formed by the laser-induced transitions; however, it is still populated as a result of the decay of the upper-lying levels, as shown by the dotted lines in the same figure. As the state $|a_{12}\rangle$ is stable with respect to both the laser-induced transitions and radiative decay, all of the population will eventually be pumped into this state. One should note, though, that as the interatomic distance goes to zero, the symmetry-breaking decay rates decrease, which leads to a corresponding increase of the required pumping time. If we choose another configuration that uses antisymmetric standing-wave geometry of the laser beams [Fig. 5(b)],

$$\alpha_{k3}=\pi, \quad \delta_{k3}=-\chi_{k3}/2, \quad |\Omega_{k3}| \ll |\chi_{k3}|, \tag{9}$$

the increase of the pumping time is still brought on by the decrease of efficiency of the symmetry-breaking laser-induced transitions at small distances since the corresponding transfer matrix elements are proportional to $|\Omega_{k3}^{(1)}-\Omega_{k3}^{(2)}|\sim\sin(\varphi_{k3}/2)$.

Strictly speaking, the above arguments hold only in the case when the RDDI coupling constants χ_{k3} on different transitions are equal (possibly up to an error on the order of γ_{k3}). This condition is satisfied, for example, when the two lower levels of the original Λ system are sublevels of the same atomic level. However, even when the RDDI coupling on two transitions differs considerably, the present treatment is still applicable provided that one uses four lasers instead of two to satisfy all of the resonance conditions for transitions shown in Fig. 5. In contrast to the methods presented in the previous sections, it is also very important to avoid a high degree of mutual coherence of the components of the biharmonic laser pumping, as otherwise the population of each atom will be trapped in a corresponding dark state [26].

To prove the foregoing arguments, we have numerically calculated the stationary states of the master equation (1) with the laser pumping parameters given by Eqs. (8) and (9). In order to disrupt trapping of the populations of the two atoms in the single-atom dark states, we introduced additional elastic dephasing of the lower level transition $|1\rangle\leftrightarrow|2\rangle$ in both atoms, which can be easily realized by the relative jitter of the two pumping laser frequencies. Assuming that this elastic dephasing is characterized by the rate Γ_{12}, the corresponding relaxation superoperator, which should be plugged into the master equation (1), has the form

$$\mathcal{L}_{\text{jitter}}\hat{\rho}=\Gamma_{12}\sum_{i,j=1,2}(2\sigma_z^{(i)}\hat{\rho}\sigma_z^{(j)}-\hat{\rho}\hat{\sigma}_z^{(i)}\hat{\sigma}_z^{(j)}-\hat{\sigma}_z^{(i)}\hat{\sigma}_z^{(j)}\hat{\rho}), \tag{10}$$

where $\sigma_z^{(i)}=n_1^{(i)}-n_{22}^{(i)}$ is the lower level population difference operator in the ith atom. For simulations we used a realistic value $\Gamma_{12}=0.01\gamma$, where we again assume for simplicity $\gamma=\gamma_{13}=\gamma_{23}$. The results of the numerical calculations of the steady state population of the level $|a_{12}\rangle$ for different values of laser pumping Rabi frequencies Ω (in our calculations they are equal for all transitions and atoms, $|\Omega_{k3}^{(i)}|=\Omega, i, k=1,2$) are presented in Fig. 6 as a function of the interatomic distance φ_{13} for the two geometries discussed. As seen from the graphs, the fidelity of the entanglement produced first monotonically decreases with increasing Rabi frequency, and then strongly degrades when the magnitude of the Rabi frequency approaches that of the RDDI splitting due to power-broadening-induced nonresonant excitation. The graphs for $\Omega=0.001\gamma$ in Fig. 6, therefore, decently represent the overall fidelity of the optical pumping method. For low Rabi frequency amplitudes, the antisymmetric geometry clearly shows better results and achieves fidelity of 0.8 at $\varphi_{13}\approx 1$, which is much better than the fidelities achieved by other methods at such distances.

V. CONCLUSIONS

We have considered three methods for creation of radiatively stable entanglement in a system of two dipole-interacting three-level atoms in a Λ configuration. It was shown that the radiatively stable maximally entangled states $|a_{12}\rangle$ and $|s_{12}\rangle$, which involve only the lower levels of the original Λ system, can be efficiently populated at small interatomic distances by employing coherent or incoherent methods.

The first of the coherent methods, which employs resonant Raman pulses for transfer of population (first to a radiatively unstable maximally entangled state and then to a stable

maximally entangled state), makes use of specific resonance conditions and symmetry-preservation rules. The second coherent method, which utilizes a STIRAP process, realizes adiabatic transfer of the population of the system into the final state coinciding with one of the radiatively stable maximally entangled states. The STIRAP method, however, requires the use of standing waves to avoid leakage of population into unentangled states.

As a rather surprising result, we have also shown that entanglement can be deterministically created as a result of an incoherent process [27], optical pumping in our case. Creating a laser field configuration where one of the maximally entangled states, $|a_{12}\rangle$ or $|s_{12}\rangle$, is not included in the chain of laser-induced transitions, we achieve high populations of that state at asymptotically large times due to radiative decay into that state. An important restriction for realization of the optical pumping method is that one has to avoid high mutual coherence of the pumping laser beams, but this restriction becomes an advantage when realizing the proposed schemes experimentally as it is usually easier to provide an incoherent pumping than a coherent one.

For two of the proposed methods (STIRAP and optical pumping), the fidelity of the created approximations of the maximally entangled states was calculated, and it shows qualitatively the same dependence on the interatomic distance R as in the previously considered two-level atom model [16]. The fidelity of 0.8 (a good benchmark for Bell inequality violations) is achieved in all of the considered methods at interatomic separations between one-fifteenth and one-sixth of the wavelengths of the working transitions.

In conclusion, we have shown that radiatively stable maximally entangled states can be created in a system of two dipole-interacting atoms under conditions that can be experimentally implemented, for example, in optical lattices [15,20]. The general form of the RDDI operator also suggests that simple analogs of the proposed methods can be employed in other physical systems, such as quantum dots in semiconductors [27,28] or cavity QED systems [24,29] (or, indeed, a combination of the latter two [30]).

ACKNOWLEDGMENTS

This work was partially supported by the programs ''Fundamental Metrology'' and ''Physics of Quantum and Wave Processes'' of the Russian Ministry of Science and Technology.

[1] See, for example, J. S. Bell, *Speakable and Unspeakable in Quantum Mechanics* (Cambridge University Press, Cambridge, 1987).
[2] For a review, see S. J. Lomonaco, Cryptologia **23**, 1 (1999).
[3] For a review, see A. Steane, Rep. Prog. Phys. **61**, 117 (1998).
[4] C. H. Bennett, G. Brassard, C. Crepeau, R. Jozsa, A. Peres, and W. K. Wooters, Phys. Rev. Lett. **70**, 1895 (1993); C. H. Bennett, D. P. DiVincenzo, J. A. Smolin, and W. K. Wootters, Phys. Rev. A **54**, 3824 (1996); H. Barnum, E. Knill, and M. A. Nielsen, e-print quant-ph/9809010.
[5] D. J. Wineland, J. J. Boilinger, W. M. Itano, and D. J. Heinzen, Phys. Rev. A **50**, 67 (1994); S. F. Huelga, C. Macchiavello, T. Pellizzari, A. Ekert, M. B. Plenio, and J. I. Cirac, Phys. Rev. Lett. **79**, 3865 (1997); A. M. Childs, J. Preskill, and J. Renes, e-print quant-ph/9904021.
[6] D. N. Klyshko, *Photons and Nonlinear Optics* (Gordon and Breach, New York, 1988).
[7] P. G. Kwiat, K. Mattle, H. Weifurter, A. Zeilinger, A. V. Sergienko, and Y. Shih, Phys. Rev. Lett. **75**, 4337 (1995); W. Tittel, J. Brendel, H. Zbinden, and N. Gisin, *ibid.* **81**, 3563 (1998).
[8] E. S. Fry, T. Walther, and S. Li, Phys. Rev. A **52**, 4381 (1995).
[9] M. B. Plenio, S. F. Huelga, A. Beige, and P. L. Knight, Phys. Rev. A **59**, 2468 (1999).
[10] C. Cabrillo, J. I. Cirac, P. Garcia-Fernandez, and P. Zoller, Phys. Rev. A **59**, 1025 (1999).
[11] D. Jaksch, H.-J. Briegel, J. I. Cirac, C. W. Gardiner, and P. Zoller, Phys. Rev. Lett. **82**, 1975 (1999).
[12] Q. A. Turchette, C. S. Wood, B. E. King, C. J. Myatt, D. Leibfried, W. M. Itano, C. Monroe, and D. J. Wineland, Phys. Rev. Lett. **81**, 3631 (1998).
[13] R. Laflamme, E. Knill, W. H. Zurek, P. Catasti, and S. V. S. Mariappan, Philos. Trans. R. Soc. London, Ser. A **356**, 1941 (1998).
[14] A. Barenco, D. Deutsch, A. Ekert, and R. Jozsa, Phys. Rev. Lett. **74**, 4083 (1995).
[15] G. K. Brennen, C. M. Caves, P. S. Jessen, and I. H. Deutsch, Phys. Rev. Lett. **82**, 1060 (1999).
[16] I. V. Bargatin, B. A. Grishanin, and V. N. Zadkov, Fortschr. Phys. (to be published).
[17] A. Beige, S. F. Huelga, P. L. Knight, M. B. Plenio, C. R. Thompson, J. Mod. Opt. **47**, 401 (2000).
[18] For a review, see D. J. Wineland, C. Monroe, W. M. Itano, D. Leibfried, B. E. King, and D. M. Meekhof, J. Res. Natl. Inst. Stand. Technol. **103**, 259 (1998).
[19] For a review, see R. Grimm, M. Weidemuller, and Y. B. Ovchinnikov, Adv. At. Mol. Opt. Phys. **42**, 95 (2000).
[20] G. K. Brennen, I. H. Deutsch, and P. S. Jessen, e-print quant-ph/9910031.
[21] G. Kurizki and A. Ben-Reuven, Phys. Rev. A **36**, 90 (1987).
[22] W. Happer, Rev. Mod. Phys. **44**, 169 (1972).
[23] For a review, see K. Bergmann, H. Theuer, and B. W. Shore, Rev. Mod. Phys. **70**, 1003 (1998).
[24] T. Pellizzari, S. A. Gardiner, J. I. Cirac, and P. Zoller, Phys. Rev. Lett. **75**, 3788 (1995).
[25] N. V. Vitanov and S. Stenholm, e-print quant-ph/9903096.
[26] For a review, see E. Arimondo, in *Progress in Optics*, edited by E. Wolf (Elsevier, Amsterdam, 1996), Vol. 35, p. 257.
[27] The idea of using incoherent processes for realization of entangling dynamics in a system of coupled quantum dots was recently considered in A. Mizel, M. W. Mitchell, and M. L.

Cohen, e-print quant-ph/9908035.
[28] G. D. Sanders, K. W. Kim, and W. C. Holton, e-print quant-ph/9909070.
[29] G. Kurizki, A. G. Kofman, and V. Yudson, Phys. Rev. A **53**, R35 (1996).
[30] A. Imamoglu, D. D. Awschalom, G. Burkard, D. P. DiVincenzo, D. Loss, M. Sherwin, and A. Small, e-print quant-ph/9904096.